Nano-scale surface morphology of magnesium anodized in a 10 M KOH electrolyte

Christopher Miller[1], Aaron F Cipriano[1], and Huinan Liu[1,2]

[1]Department of Bioengineering
[2]Materials Science and Engineering Program

ABSTRACT

Magnesium (Mg) is a promising implant material for orthopedic applications due to its biodegradability and desirable mechanical properties. However, in order for Mg to have wide-spread clinical relevance, engineering solutions that address the rapid degradation in physiological environments and promote increased bone-forming activity are necessary. The objective of this study was to develop an anodization process using a toxicant-free electrolyte to modulate nano-scale surface features and surface chemistry on Mg. Anodic polarization and potentiostatic anodization tests were used to evaluate the effect of applied potential on surface morphology of Mg in a 10 M KOH electrolyte. The alkaline electrolyte used for anodization of Mg in this study offers an alternative to commercial processes that use highly toxic elements. The anodized samples were annealed to investigate the effect of thermal treatments on surface morphology and chemical composition. The nanostructure and chemical composition of the anodized and annealed Mg substrates were characterized using a scanning electron microscope and energy dispersive X-Ray Spectroscopy. Our results showed that the nanostructures and chemical composition of anodically-generated oxide layers on Mg are specific to each oxidation process in a 10 M KOH electrolyte. Our results begin to suggest the possibility to rationally design the surface features at the nano-scale and improve the corrosion resistance of bulk Mg.

Keywords: Oxidation of magnesium, potentiostatic anodization, nanostructure, annealing

FACULTY MENTOR

Huinan Liu

Department of Bioengineering,
Department of Material Sciences and Engineering,
UCR Stem Cell Center

Professor Liu's research is to understand cell-biomaterial and tissue-biomaterial interactions in 2D and 3D and to develop better tissue substitutes and medical implant materials using biodegradable polymers, ceramic nanoparticles, polymer/ceramic nanocomposites and bioresorbable metals.

AUTHOR

Christopher Miller

Bioengineering

Christopher Miller is a Junior in Bioengineering. He has participated in undergraduate research in Dr. Huinan Liu's laboratory, the Biomaterials and Nanomedicine Laboratory, since January 2012. Throughout his time in Dr. Liu's laboratory he has developed an interest in nanotechnology and regenerative medicine. He has worked closely with Aaron Cipriano, a PhD. candidate in Dr. Liu's lab, on several projects focused on improving Magnesium's potential as an orthopedic implant material. Together they have developed an electrochemical anodization process through which Chris aims to generate a corrosion-resistant and biocompatible Magnesium Oxide layer on the surface of Magnesium substrates for orthopedic applications. He is a participant in UC Riverside's Honors Program and Tau Beta Pi chapter, California Alpha Beta. His accolades include selection to the Student Editorial Board of UCR's Undergraduate Research Journal Volume VII, selection for participation in the prestigious *UC LEADS* program, and receiving the Outstanding Achievement Award from UCR's Bourns College of Engineering. He plans to pursue a PhD in Bioengineering and a career in industry.

Christopher Miller

1. INTRODUCTION

Currently, non-degradable metals, such as Titanium (Ti) and its alloys, are commonly used materials for orthopedic fixation devices [1]. However, the permanency of these metals in the body after healing of the tissue has occurred can cause stress-shielding due to their high elastic modulus, interfere with bone growth in pediatric patients, and require subsequent surgery for removal and repair [2]. Alternatively, the use of bioabsorbable polymers for orthopedic fixation devices, such as poly-L-lactide (PLA), has been introduced to eliminate the need for surgeries for removal of idle implants. However, these polymers usually exhibit inferior mechanical properties and produce acidic degradation products that lead to device breakage and inflammation of surrounding tissue [3, 4].

Mg and Mg-based alloys hold promise to address the limitations associated with current materials used for orthopedic fixation devices due to their controllable degradation, desirable mechanical properties and the body's ability to metabolize Mg degradation products [5-7]. Table 1 summarizes the mechanical properties of cortical bone, Mg, Ti alloy and PLA, and it is seen that Mg has an elastic modulus closer to cortical bone than Ti and greater tensile strength than PLA.

Table 1: *Elastic Modulus and Tensile Strength of cortical bone, Mg, Ti alloys and PLA [8].*

Mechanical Property	Cortical Bone	Mg	Ti alloys	PLA
Elastic Modulus (GPa)	3-20	41-45	110-117	2.2-9.5
Tensile Strength (MPa)	100-200	230-250	730-950	16-69

However, in order to promote osseointegration of Mg-based implants, it is also vital to generate implants with surface morphology at the nanoscale. Studies have shown that osteoblasts and osteoclasts, bone-forming and bone-resorbing cells respectively, show enhanced function on nanoscale surface features [9, 10]. Bone metabolism consists of coordinated functions of osteoblasts and osteoclasts, and enhanced activity of these cells is therefore highly desired in the area surrounding orthopedic implants [11]. Furthermore, competitive cells such as fibroblasts, which promote fibrous encapsulation and callus formation events that can lead to implant loosening and failure, have been shown to be inactivated by nanoscale surface features [12]. Therefore, a challenge in the development of Mg implants for clinical use resides in rationally engineering surface morphologies at the nanoscale with processes that do not include elements that could induce systemic toxicity in the human body.

2. CONCEPTUAL DEVELOPMENT

In this study we investigated the use of potentiostatic anodization of Mg in a non-toxic electrolyte to engineer surface morphologies at the nanoscale. Anodization has been shown to be a versatile electrochemical process used to generate protective oxide layers with tailored microstructures on several metals, including Mg and Mg alloys [13-15]. We used an aqueous alkaline solution of KOH, which has been reported to generate anodic oxide layers on Mg alloys [15]. This electrolyte is notably free of toxic and hazardous compounds commonly used in anodization, e.g. chromates, fluorides [16, 17]. Depending on the applied anodization potential (and resulting current density, J), Mg can exhibit one of the following processes: cathodic, which leads to active metal dissolution to Mg^{+} ions; passivation, which leads to formation of Mg hydroxide ($Mg(OH)_2$); secondary oxidation, which leads to the formation of Mg oxide (MgO); and transpassive, which results from a competition between secondary oxidation and transpassive dissolution [18]. The objective of this study was to investigate the surface morphology of Mg after potentiostatic anodization in a 10 M KOH electrolyte for 2 hr at applied potentials representative of the distinct processes (e.g. passive, secondary oxidative, transpassive). Furthermore, we investigated the effect of annealing at 450°C for 6 hr on the surface morphology and composition, and elemental distribution.

3. MATERIALS AND METHODS

3.a Mg Substrate Preparation and Characterization

Pure Mg as-rolled sheets with a thickness of 1 mm (Alfa Aesar, 99.95%) were cut into 1 x 0.5 cm rectangles. The samples were mechanically rough polished using sequential increments of 600, 800 and 1200 grit silicon

carbide abrasive papers (Ted Pella, Inc.) to remove surface oxides. The samples were subsequently fine polished using sequential increments of 6 µm, 3 µm, 1 µm and 0.25 µm diamond pastes (Physical Test Solutions) applied with a polishing pad (KEMPAD, Allied High Tech Products) to remove surface defects. Each polished pure Mg (PP-Mg) sample was subsequently ultrasonically cleaned (VWR, Model 97043-036) for 15 min in separate baths of 200-proof ethanol and acetone (Sigma-Aldrich) prior to anodization.

3.b Electrochemical Tests

All electrochemical tests were performed using a potentiostat (Model 273A, Princeton Applied Research) and current was recorded using a digital multimeter (GDM-8251A, GWInstek) interfaced with a desktop PC. The PP-Mg working electrode was connected to a copper contact using a custom-made electrode holder that exposed a surface area of 0.65 cm^2. Platinum foil placed cylindrically around the PP-Mg was used as a counter electrode and a silver/silver chloride ($Ag/AgCl_2$) electrode was used as a reference. All electrolytes consisted of a 10 M KOH solution prepared using deionized water and analytical-grade reagents. All experiments were carried out at room temperature.

Anodic Polarization of PP-Mg: In order to identify the oxidation processes of PP-Mg in a 10 M KOH solution, and therefore identify anodization potentials that could lead distinct surface morphologies, a linear potential sweep from -2 V to +2 V was performed at a rate of 3 mV/s.

Potentiostatic anodization of PP-Mg: Anodization was carried out at constant voltages that represented distinct oxidation processes of PP-Mg in a 10 M KOH electrolyte: 0.5 V (secondary oxidation process), 1.5 V and 2.0 V (transpassive oxidation process). These samples were termed A-Mg0.5, A-Mg1.5, and A-Mg2 respectively. All anodization processes had a duration of 2 hr and stirring to ensure homogeneity of the electrolyte and. The current generated during potentiostatic anodization was recorded to study the current density response to the formation of surface oxide layers [18, 19]. The anodized samples were subsequently ultrasonically cleaned in 200-proof ethanol for 15 min and dried in air prior to characterization.

3.c Annealing of A-Mg0.5, A-Mg1.5, and A-Mg2

The anodized samples were annealed at 450º C for 6 hr using an inductive furnace (F47915, Thermo Scientific) controlled by a microcontroller (Micromega, Omega Engineering) to convert $Mg(OH)_2$ surface layers to MgO by a dehydration reaction. The annealing cycle consisted of an initial heating ramp of 100°C/hr to 450°C followed by 6 hr at the set temperature and cooling to room temperature. Annealed A-Mg samples were termed AA-Mg.

3.d Characterization of PP-Mg, A-Mg and AA-Mg

Optical photographs of PP-Mg, A-Mg, and AA-Mg samples were obtained to show notable differences to the naked eye of the anodized layers. Surface morphology was characterized using a scanning electron microscope (SEM; Philips XL30) and surface elemental composition (atomic percentage, or at.%) was determined using energy dispersive X-ray spectroscopy (EDS).

4. RESULTS AND DISCUSSION

4a. Characterization of PP-Mg

Results from the characterization of PP-Mg are described in Figure 1. After preparation, the surface of the Mg was

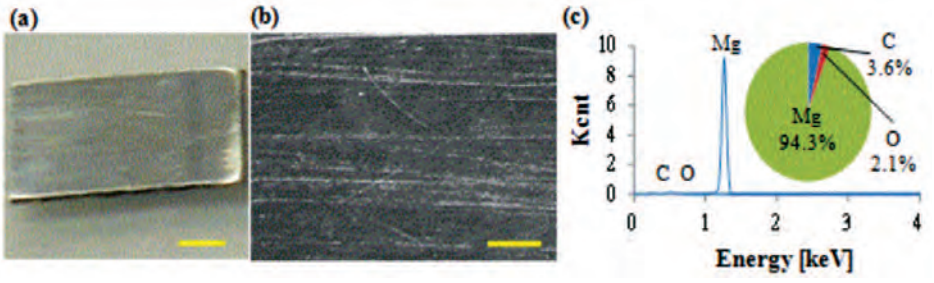

Figure 1: PP-Mg substrate used for anodization. (a) Optical photograph, scale bar = 1 mm; (b) SEM image, scale bar = 50 µm; and (c) EDS spectra and elemental composition (at. %).

shiny with polishing marks on the surface (Figure 1a). The polishing marks were also observed in the SEM images obtained at 1,000x magnification (Figure 1b). EDS analysis of the PP-Mg surface showed trace amounts of oxygen (O) and carbon (C) content, 2.1 (at.%) and 3.6 (at. %), respectively. Fine polishing of PP-Mg removed surface defects, which was highly desired to ensure uniform coverage of anodic oxide surface features [20].

4b. Electrochemical tests

Anodic polarization of PP-Mg: Figure 2 shows the anodic polarization plot obtained for the behavior of PP-Mg in a 10 M KOH electrolyte. Four distinct regions which indicated unique oxidation processes that occurred during potentiostatic anodization were observed. Region A indicated a cathodic process (- 2 V to -0.7 V), Region B indicated passivation (-0.7 V to -0.1 V), Region C indicated secondary oxidation (-0.1 V to +0.9 V), and Region D indicated transpassive process (+0.9 V to +2 V). The four regions observed in Figure 2 indicated that the anodic oxidation of Mg in a 10M KOH electrolyte is characteristic of an active-passive metal [18]. The four regions in the anodic polarization curve identified regions which could lead to distinct anodically-generated surface morphologies with different surface chemistries. To the best of the authors' knowledge, the relationship between surface morphology and anodization in different regions of a polarization curve for PP-Mg in a highly alkaline electrolyte has not been reported previously in literature.

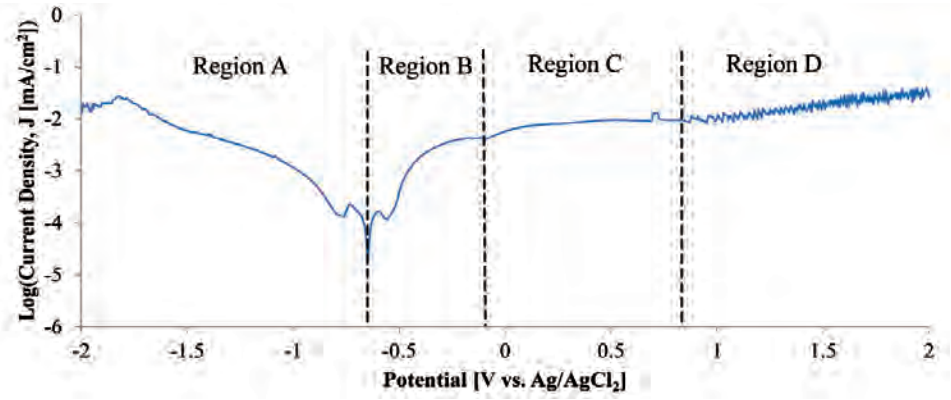

Figure 2: *Anodic polarization plot of PP-Mg in 10M KOH solution at a scan rate of 3 mV/s.*

The degradation of Mg in physiological fluids is rapid. The degradation of Mg involves the conversion of Mg^{+} ions to $Mg(OH)_2$, followed by the conversion of the hydroxide to soluble Mg chloride ($MgCl_2$). Therefore, in physiological fluids, where chloride ions (Cl^-) are abundant, the degradation of Mg is rapid. One of the reaction products from the conversion of $Mg(OH)_2$ to $MgCl_2$ is the formation of excess hydroxide ions, which can lead to a harmful increase in local pH levels [21]. Conversely, MgO films are more stable and help improve the corrosion properties of Mg [21]. Therefore, in order to generate MgO barrier-type films with nano-scale features, we focused on anodizing at potentials in Regions C and D. Furthermore, in order to ensure generation of MgO films, we annealed the A-Mg samples at 450ºC for six hr to convert $Mg(OH)_2$ to MgO via a dehydration reaction [22].

Anodization of PP-Mg: Figure 3 shows a plot with the current densities, J, resulting from potentiostatic anodization processes in a 10 M KOH electrolyte for 2 hr to generate A-Mg0.5, A-Mg1.5, and A-Mg2. The current density observed for A-Mg0.5 featured an initial peak that reached a value of 8.71 mA/cm^2 (Figure 3, inset) and was followed by a gradual decrease to a current density of 0.028 mA/cm^2. This initial peak followed by a decrease in current density has been reported to be indicative of passivation/secondary oxidation [23]. The curves for A-Mg1.5 and A-Mg2 produced an oscillating current density response with the oscillations centering at current densities of 16 mA/cm^2 and 70 mA/cm^2, respectively. These oscillations were indicative of the periodic cycle composed of passivation/oxidation followed by destruction of the oxide layer, which is characteristic of transpassive processes. Bubble evolution was observed on the surface of the platinum counter electrode during A-Mg1.5 and A-Mg2 synthesis, which was a sign of the O_2 gas evolution expected with transpassive dissolution.

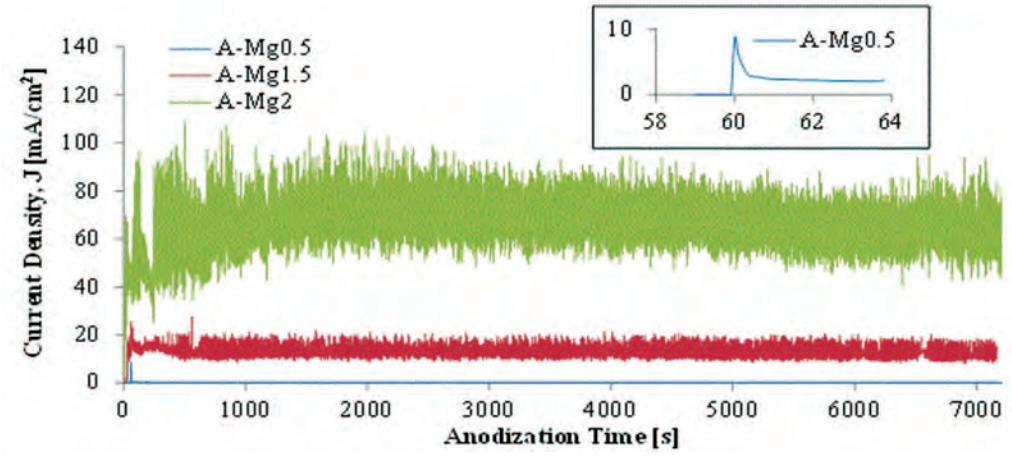

Figure 3: *Current density during potentionstatic anodization in 10M KOH of A-Mg0.5, A-Mg1.5, and A-Mg2. Inset is a magnification of the initial current density peak observed during the anodization of A-Mg0.5.*

4c. Characterization of A-Mg and AA-Mg

Optical photographs and results from SEM/EDS analysis of A-Mg are shown in Figure 4. Figures 4a-c show optical photographs where the differences in surface morphology were notably different. In terms of surface appearance to the naked eye, A-Mg0.5 had a dark-gray hue, A-Mg1.5 appeared gray with a tarnished region in the center, and A-Mg2 appeared to have a light-gray color. A lack of a metallic sheen and scratches on the surface was observed on the surface of all three substrates. The SEM images shown in Figures 4d-f (1,000x magnification) for A-Mg0.5, A-Mg1.5, and A-Mg2 respectively, indicated that distinct surface morphologies were obtained for anodization in different oxidation regions of the anodic polarization plot of PP-Mg. For example, nucleating structures were observed on A-Mg1.5 (white regions in Figure 4e), while A-Mg2 had a relatively homogenous anodic film.

EDS analysis, shown in Figures 4g-i, revealed differences in O content in the varying oxide features present on these samples. Oxygen content increased with applied potential;

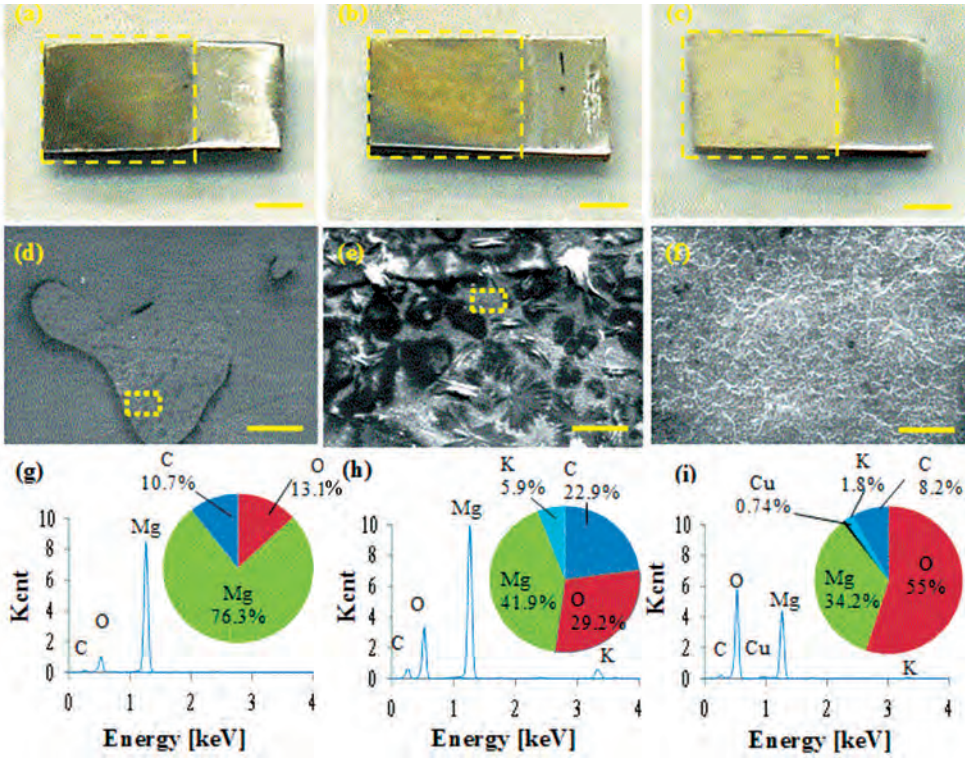

Figure 4: *Anodized Mg in 10 M KOH aqueous electrolyte for 2 hr at applied potentials of 0.5 V, 1.5 V, and 2 V. Optical photographs of (a) A-Mg0.5, (b) A-Mg1.5, and (c) A-Mg2, scale bar = 1 mm; anodized region outlined by dashed-lines. SEM images of (d) A-Mg0.5, (e) A-Mg1.5, and (f) A-Mg2, scale bar = 50 µm. (g)-(i) EDS spectra and elemental composition (at. %) of (d) in the dashed-line region, (e) in the dashed line region, and (f) respectively.*

Christopher Miller

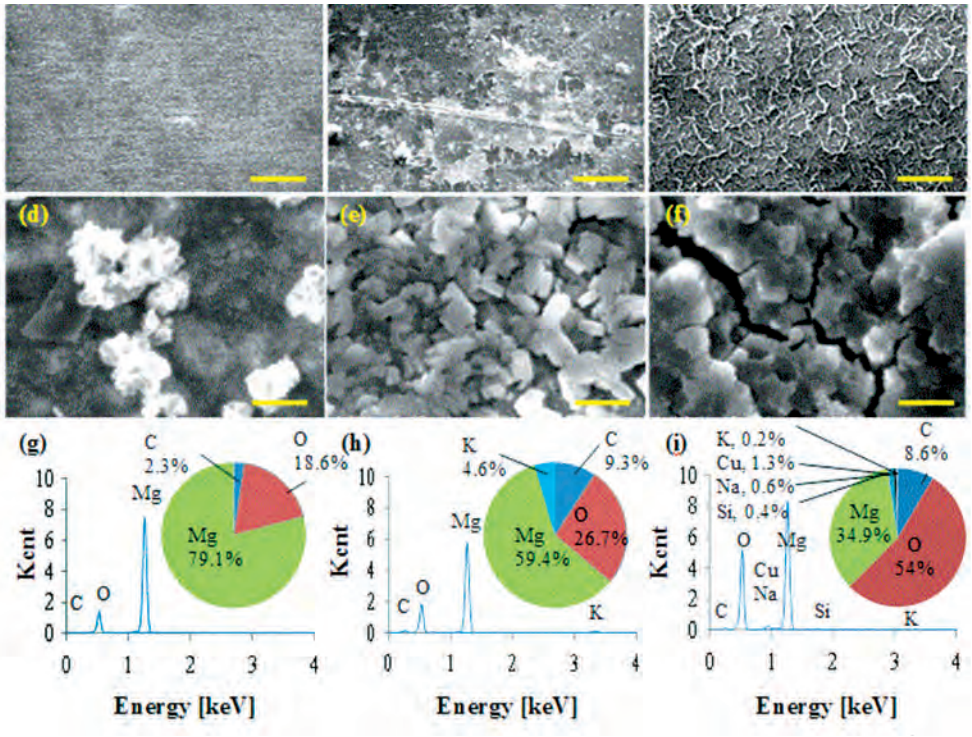

Figure 5: *Anodized Mg in 10 M KOH aqueous electrolyte for 2 hr at applied potentials of 0.5 V, 1.5 V, and 2 V and annealed at 450°C for 6 hr. SEM images of (a) AA-Mg0.5, AA-Mg1.5, and AA-Mg2, scale bar = 50 µm; and (d) AA-Mg0.5, (e) AA-Mg1.5, and (f) AA-Mg2, scale bar = 500 nm; and (g) – (i) EDS spectra and surface elemental composition (at. %) of (d) – (f), respectively.*

specifically, 13.1, 29.2 and 55 at. % for A-Mg0.5, A-Mg1.5, and A-Mg2, respectively. As a result, the O/Mg at. % ratio had values of 0.17, 0.70, and 1.6 for the A-Mg0.5, A-Mg1.5, and A-Mg2, respectively. An approximate ratio of O/Mg equal to 2, observed on A-Mg2, was an initial indicator of the presence of $Mg(OH)_2$ on the surface. Increased O content was observed in all A-Mg samples as compared with PP-Mg. The presence of potassium (K) on the surface of A-Mg samples was attributed to residual K^- ions from the electrolyte. The traces of copper (Cu) were attributed to contamination from the electrical contacts used during anodization.

SEM images and EDS spectra for the AA-Mg samples are shown in Figure 5. SEM analysis at a 1,000x magnification showed that the surface features on AA-Mg0.5 became homogenized as compared with A-Mg0.5 (Figure 5a). It was observed that the nucleating oxide structures of A-Mg0.5 became homogenized in AA-Mg0.5 (Figure 5b). The surface morphology of AA-Mg2 appeared unchanged when compared with A-Mg2 (Figure 5c). SEM analysis at 100,000x magnification of the AA-Mg0.5, AA-Mg1.5, and AA-Mg2 (Figures 5d-f, respectively) showed that each applied potential followed by annealing, produced unique nanoscale surface morphologies. The homogeneity of the nanoscale features was observed to be greater on the AA-Mg1.5 and AA-Mg2 than on AA-Mg0.5. Surface cracks were observed in the nanostructure of AA-Mg2, which were indicative of defects in the anodically generated oxide layer.

EDS spectra and elemental composition summarized in Figures 4g-i showed that the O/Mg at. % ratios remained relatively constant on all three samples after annealing, specifically 0.24, 0.44, and 1.55 on AA-Mg0.5, AA-Mg1.5, and AA-Mg2, respectively. This indicated that the conditions for a dehydration reaction to take place with $Mg(OH)_2$ were not met for all A-Mg samples. Therefore, we speculated the most Mg present on the surface was in a metallic form with smaller amounts in the form of MgO. Traces of C on the surfaces of the AA-Mg0.5 and AA-Mg1.5 decreased compared with values observed on their A-Mg counterparts. Conversely, the amount of Mg increased for these same AA-Mg samples compared with their A-Mg counterparts. This indicated that annealing eliminated some of these contaminants from the anodically-generated layer. The amount of C and Mg on AA-Mg2 remained relatively unchanged as compared with A-Mg2. Additionally, trace amounts of sodium (Na) and silicon (Si), possibly introduced as contaminants during annealing, were present on AA-Mg2.

5. Conclusions

Anodic oxide layers were generated on the surface of bulk Mg by potentiostatic anodization in a 10M KOH electrolyte for 2 hr at various applied potentials followed by annealing at 450 ºC for 6 hr. The alkaline electrolyte used for anodization of Mg in this study offers an alternative to commercial processes that use highly toxic elements. Our results show that the generated oxide layers feature unique surface nanostructure and elemental composition and distribution depending on the anodization applied potential (i.e., Mg oxidation process). EDS results before and after annealing indicate that the surface composition is a mix of metallic Mg and MgO. The ability to tailor the nanoscale morphology of these anodic layers by altering anodization parameters could lead to inexpensive procedures to enhance Mg's bioactivity. Our results showed that an applied potential of 2V followed by annealing for 6 hr at 450ºC yielded greatest homogeneity of nanoscale surface features. Additional studies are necessary to elucidate the crystal structure and stoichiometry of surface compounds. Future work includes an iterative methodology to optimize anodization parameters through which we can generate thick, barrier type MgO films with homogenous nanoscale surface features.

ACKNOWLEDGEMENTS:

The authors would like to thank the Dr. Huinan Liu for mentoring; UC Riverside and the Liu Research Group for financial and academic support; and, the Central Facility for Advanced Microscopy and Microanalysis at UC Riverside for SEM and EDS.

REFERENCES

[1] Uhthoff H, et al. D. J. Orthop Sci. 2006;11:118-26.

[2] Shen C, et al. Arthroscopy. 2010;26:705-13.

[3] Beevers DJ. Proc Inst Mech Eng H. 2003;217:59-75.

[4] Smith CA, et al. Arthroscopy. 2003;19:E115-17.

[5] Staiger M, et al. Biomaterials. 2006;27:1728–34.

[6] Hort N, et al. Acta Biomater. 2010;6:1714-25.

[7] Witte F. Acta Biomater. 2010;6:1680-92.

[8] Liu H. Nanotech Enabled In Situ Sensors for Monitoring Health; 2011. p. 115-37.

[9] Webster T, et al. Biomat. Res. 1999;20:1221–7.

[10] Webster TJ, et al. Biomaterials. 2000;21:1803-10.

[11] Webster T, et al. Biomaterials 2001;22:1327–33.

[12] Vance R, et al. Biomaterials 2004;25:2095–103.

[13] Tsuchiya H, et al. Corrosion Science. 2005;47: 3324–35.

[14] Macdonald DD. J Electrochem Soc. 1993; 140:L27-L30.

[15] Lei T, et al. Surface and Coatings Technoogy. 2010;204:3798–803.

[16] Koji Murakami, et al. Magnesium Alloys - Corrosion and Surface Treatments: 2011.

[17] Bauer S, et al. Electrochemistry Communications. 2006;8:1321–5.

[18] Cai Z, et al. Internation Journal of Hydrogen Energy. 2009;34:467-72.

[19] Lei T, et al. Corrosion Science. 2010;52:3504–8.

[20] Dale GR, et al. J Nanosci Nanotechnol. 2009;9: 4215-9.

[21] Li Z, et al. Biomaterials. 2008;29:1329-44.

[22] Yoshida T, et al. J Phys Chem. 1995;99:10890-6.

[23] Kang S, et al. Journal of Industrial and Engineering Chemistry. 2008;14:52-9.